All-optical format conversion using a periodically poled lithium niobate waveguide and a reflective semiconductor optical amplifier

Jian Wang,[a] Junqiang Sun,[b] Qizhen Sun, Dalin Wang, Minjuan Zhou, Xinliang Zhang, and Dexiu Huang
Wuhan National Laboratory for Optoelectronics, School of Optoelectronic Science and Engineering, Huazhong University of Science and Technology, Wuhan, 430074 Hubei, People's Republic of China

M. M. Fejer
Edward L. Ginzton Laboratory, Stanford University, Stanford, California 94305

(Received 21 March 2007; accepted 28 June 2007; published online 31 July 2007)

In the present letter, the authors report on the realization of all-optical format conversion by using the cascaded sum- and difference-frequency generation in a periodically poled lithium niobate waveguide and the active mode locking in a reflective-semiconductor-optical-amplifier-based fiber ring laser. Tunable format conversions from nonreturn-to-zero pseudorandom binary sequence (PRBS) signal to return-to-zero PRBS idler at 10 and 20 Gbit/s are observed in the experiment. © *2007 American Institute of Physics*. [DOI: 10.1063/1.2761513]

Quasiphase matched (QPM) periodically poled lithium niobate (PPLN) waveguide has attracted considerable interest in high-speed all-optical signal processing due to its distinct advantages of high nonlinear coefficient, ultrafast nonlinear optical response, no excess noise, and versatile second-order nonlinearities and their cascading.[1] During the past few years, various nonlinear applications including efficient all-optical wavelength conversions,[2–7] optical pulse compression,[8] and all-optical logic gates[9–12] have been proposed and demonstrated based on the PPLN waveguides. Typically, these previous researches mostly focused on the nonlinear interactions between either continuous-wave (cw) lights[2,3] or pulsed lights,[4–7] or data streams.[10,11] Recently, we have suggested and numerically simulated a PPLN-based application of all-optical format conversion by employing a data stream and a pulsed light.[13,14] Note that, owing to the capability of connecting different networks which employ various data formats with each other, all-optical format conversion is also regarded as one of the important functions for future reconfigurable all-optical networks. For example, all-optical format conversion between nonreturn-to-zero (NRZ) and return-to-zero (RZ) is an important interface technology for future optical networks that employ both wavelength-division-multiplexing and optical-time-division-multiplexing technologies. However, the experimental demonstration on PPLN-based all-optical format conversion has not yet been reported up to now. In this letter, we propose and experimentally demonstrate a scheme to perform all-optical format conversion from NRZ to RZ by using a PPLN waveguide and a reflective semiconductor optical amplifier (RSOA). With the pulsed optical clock generated from the RSOA-based actively mode-locked fiber ring laser (AMLFRL), based on the cascaded sum- and difference-frequency generation (cSFG/DFG) between NRZ signal and such optical clock in the PPLN waveguide, 10 and 20 Gbit/s tunable NRZ-to-RZ format conversions for the pseudorandom binary sequence (PRBS) NRZ signal are observed in the experiment.

Figure 1 schematically shows the experimental setup for PPLN+RSOA-based all-optical format conversion, which can be divided into four parts (I–IV): the NRZ signal generator, the NRZ-to-pseudoreturn-to-zero (PRZ) converter, the all-optical clock recovery unit, and the NRZ-to-RZ converter. In part I, the NRZ signal is generated by using a tunable laser (TL), a Mach-Zehnder modulator (MZM), a bit pattern generator (BPG), a tunable frequency synthesizer (TFS), and an erbium-doped fiber amplifier (EDFA1). In order to clearly observe the bit patterns for NRZ-to-RZ format conversion later in the experiment, 2^7-1 PRBS NRZ signal is employed. In part II, the PRBS NRZ signal with weak clock components is converted into PRZ signal to enhance the clock components by using a fiber delay interferometer (FDI). The FDI is constructed with two 3 dB couplers (C2 and C3) and two fiber arms with a length difference of 5.2 mm, resulting in a time delay of 25 ps (Δt). The operation temperature of the lower arm is controlled by a temperature controlling block (TCB) to adjust the phase shift ($\Delta\varphi$). Such a simple FDI can perform NRZ-to-PRZ format conversion for 10 and 20 Gbit/s NRZ signals. In part III, the all-optical clock recovery from PRZ signal with enhanced clock components is able to be achieved easily using a RSOA-based AMLFRL. The AMLFRL consists of a variable optical attenuator (VOA1), a 3 dB coupler (C5), a polarization controller (PC1), a RSOA with better modulation performance compared with conventional SOA, a circulator, a tunable delay line (TDL1), an isolator (ISO), a tunable filter (TF1), and a 10:90 coupler (C6). The PRZ signal is injected into the fiber ring laser with its power controlled by VOA1. The gain of the ring cavity is provided by a 1000 μm strained, multiquantum-well (MQW) InGaAsP–InP material RSOA. Its small-signal gain is 18 dB with the peak gain wavelength at 1550 nm when biased at 200 mW. The isolator is used to ensure the unidirectional oscillation in the ring cavity. TF1 with a 3 dB bandwidth of 1 nm is used to select the wavelength of the recovered optical clock. The length of the ring cavity can be changed by tuning TDL1. By carefully adjusting VOA1, PC1, and TFS or TDL1 in the ring cavity, it is possible to generate stable optical clock. In part IV, the extracted optical clock serving as the pulsed pump (λ_P), together with the input NRZ signal (λ_S) and cw control (λ_C)

[a]Electronic mail: wjhustoe@163.com
[b]Eletronic mail: jqsun@mail.hust.edu.cn

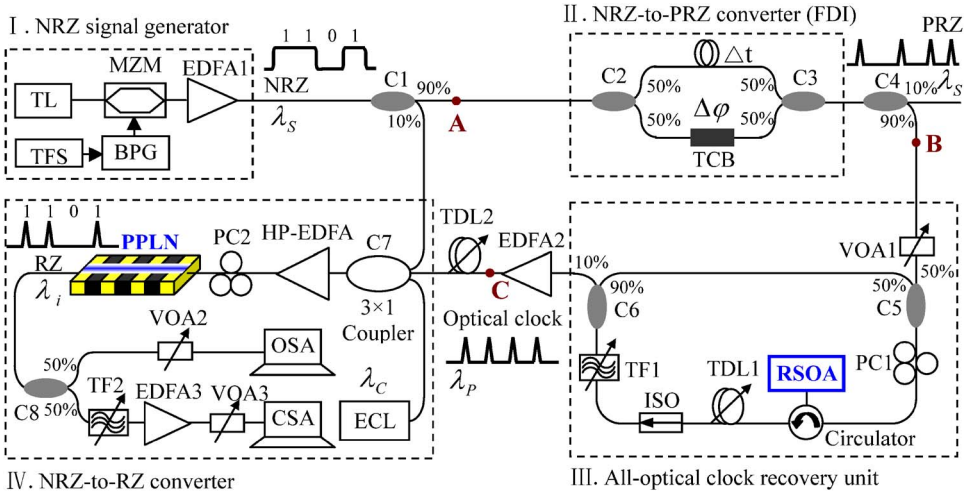

FIG. 1. (Color online) Schematic diagram of the experimental setup for PPLN+RSOA-based all-optical NRZ-to-RZ format conversion.

emitted from the external cavity laser (ECL) are combined by a 3×1 coupler (C7), amplified by a high-power EDFA (HP-EDFA) with a small-signal gain of 40 dB and a saturation output power of 30 dBm, and then launched into the PPLN waveguide to participate in the cSFG/DFG nonlinear interactions. During the cSFG/DFG processes, the NRZ signal and the pump optical clock are used to yield the sum-frequency wave under the SFG QPM condition. At the same time, the cw control interacts with the sum-frequency wave to generate the idler wave through the subsequent DFG process. Note that the converted idler can be obtained only when all the three waves (NRZ signal, pump optical clock, and cw control) are present, which corresponds to the NRZ-to-RZ format conversion from the signal wave to the idler wave. A 50-mm-long PPLN waveguide fabricated by the electric-field poling method and annealing proton-exchanged (APE) technique is used in the experiment. It has a microdomain period of 14.7 μm, a waveguide width of 12 μm, an initial proton exchange depth of 0.8 μm, and a QPM wavelength of 1543.2 nm at room temperature. The fiber-to-fiber coupling loss of the PPLN waveguide is estimated at about 4.7 dB due to the reflection losses at the uncoated end faces, mode mismatching between the fibers and the waveguide, and intrinsic waveguide losses. PC2 is used to adjust the polarization state of input optical waves before entering into the PPLN waveguide. TDL2 is employed to adjust the time delay between the NRZ signal and the pump optical clock. The optical spectra are monitored by an optical spectrum analyzer (OSA, Anritsu MS9710C) with the highest spectral resolution of 0.05 nm, and the bit patterns are observed through a communications signal analyzer (CSA, Tektronix 8000B).

Figure 2 depicts the measured optical spectra for NRZ-to-PRZ format conversion. As shown in Fig. 2(a), it is found that the FDI acts as a comb filter which has a wavelength spacing of 0.32 nm. In the experiment, the operation temperature of the FDI is properly controlled so as to move one notch aiming at the center wavelength of the input NRZ signals. As a result, 10 and 20 Gbit/s input NRZ signals, as shown in Figs. 2(b) and 2(d), are respectively, converted into the corresponding PRZ signals after passing through the FDI, which can be seen from Figs. 2(c) and 2(e). Remarkably, there appear two main modes with the mode spacings of 0.08 nm (10 GHz) for 10 Gbit/s in Fig. 2(c) and 0.16 nm (20 GHz) for 20 Gbit/s in Fig. 2(e) in the optical spectra of converted PRZ signals. Thus the clock components can be greatly enhanced with the help of the NRZ-to-PRZ format conversion.

Figure 3 illustrates the measured optical spectra for cSFG/DFG-based NRZ-to-RZ format conversion at 10 Gbit/s. The wavelength of the input NRZ signal is tuned at 1546.8 nm. The wavelength of the pump optical clock is adjusted at 1539.3 nm by tuning TF1 in the AMLFRL in order to satisfy the SFG QPM condition. As shown in Fig. 3(a), when the control wavelength is tuned at 1550.8 nm, the new generated RZ idler wave can be obtained at 1535.5 nm. Additionally, as can be seen from Fig. 3(b), even for a fixed input NRZ signal, it is possible to change the wavelength of the converted RZ idler simply by the variation of the cw control wavelength. According to the previous theoretical analyses,[13] the output RZ idler can be tuned in a wide wavelength range larger than 60 nm. Thus tunable operation of NRZ-to-RZ format conversion can be easily performed.

To further confirm the PPLN+RSOA-based NRZ-to-RZ format conversion, the bit patterns for different optical waves (2^7-1 PRBS) are observed. As shown in Fig. 4(a), R1–R4, respectively, represent 10 Gbit/s input PRBS NRZ signal (point A in Fig. 1), PRZ signal (point B in Fig. 1), pump optical clock (point C in Fig. 1), and output RZ idler corre-

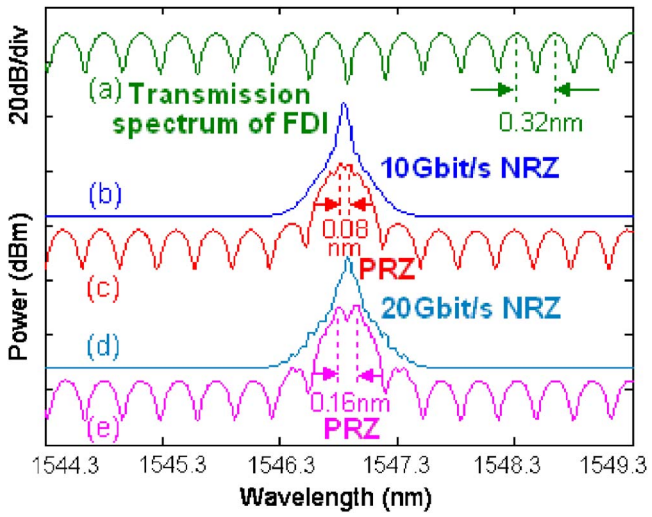

FIG. 2. (Color online) Measured optical spectra for NRZ-to-PRZ format conversion. (a) Transmission spectrum of FDI and the resulting specta of [(b) and (d)] NRZ and [(c) and (e)] PRZ at [(b) and (c)] 10 Gbit/s and [(d) and (e)] 20 Gbit/s.

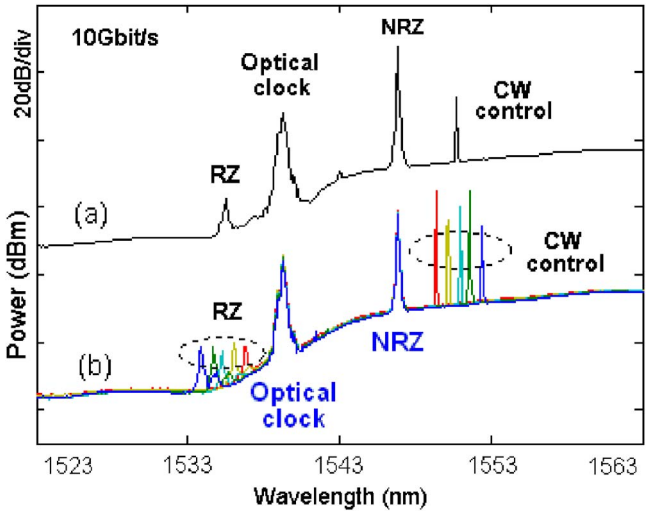

FIG. 3. (Color online) Measured optical spectra for cSFG/DFG-based NRZ-to-RZ format conversion at 10 Gbit/s. (a) cw control is tuned at 1550.8 nm. (b) Tunable operation under different control wavelengths of 1549.4, 1550.2, 1551.0, 1551.6, and 1552.4 nm.

sponding to Fig. 3(a). It is apparent that, NRZ-to-PRZ format conversion (R1 and R2), all-optical clock recovery (R2 and R3), and NRZ-to-RZ format conversion (R1 and R4) are all implemented. Figure 4(b) illustrates the tunable NRZ-to-RZ format conversion at 10 Gbit/s. R5–R9 plot the bit patterns for tunable output RZ idlers corresponding to Fig. 3(b) under different control wavelengths of 1549.4, 1550.2, 1551.0, 1551.6, and 1552.4 nm, respectively. No obvious changes are observed during the tuning process. The scales in Figs. 4(a) and 4(b) are 500.0 ps/division. Figure 4(c) shows the bit patterns for NRZ-to-RZ format conversion operating at 20 Gbit/s. The scale in Fig. 4(c) is 200.0 ps/division. R10–R13 depict 20 Gbit/s input PRBS NRZ signal (point A in Fig. 1), PRZ signal (point B in Fig. 1), pump optical clock (point C in Fig. 1), and output RZ idler, respectively. It can be clearly seen that 20 Gbit/s NRZ-to-RZ format conversion (R10 and R13) is also realized with the proposed scheme.

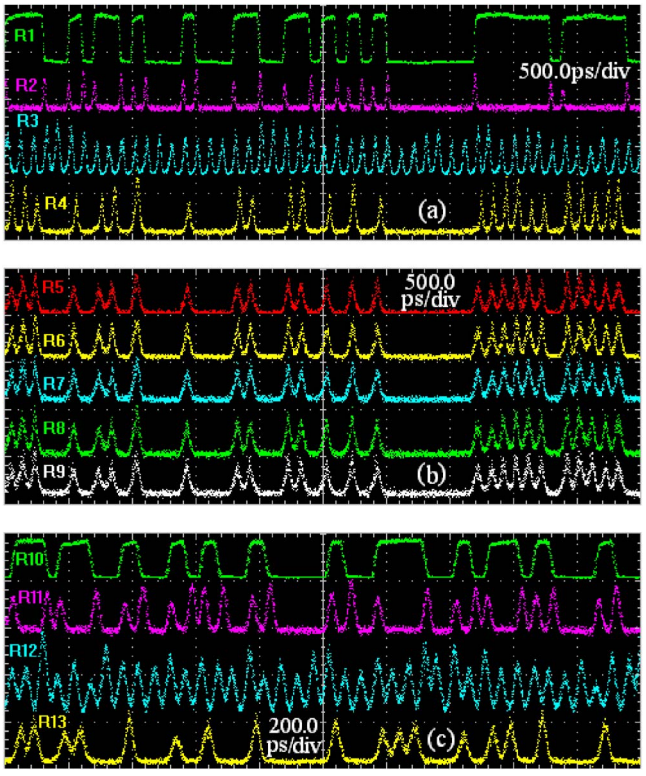

FIG. 4. (Color online) Measured bit patterns for 10 and 20 Gbit/s tunable NRZ-to-RZ format conversion. (a) 10 Gbit/s NRZ-to-RZ format conversion corresponding to Fig. 3(a). R1: input NRZ signal at point A in Fig. 1. R2: PRZ signal at point B in Fig. 1. R3: pump optical clock at point C in Fig. 1. and R4: output RZ idler with the control wavelength set at 1550.8 nm. (b) Tunable operation at 10 Gbit/s corresponding to Fig. 3(b). R5–R9: tunable output RZ idlers with different control wavelengths of 1549.4, 1550.2, 1551.0, 1551.6, and 1552.4 nm, respectively. (c) 20 Gbit/s NRZ-to-RZ format conversion. R10: input NRZ signal at point A in Fig. 1. R11: PRZ signal at point B in Fig. 1. R12: pump optical clock at point C in Fig. 1. R13: output RZ idler with the control wavelength set at 1551.2 nm.

With further improvement, two future potential applications can also be implemented with our proposed scheme. First, it is possible to perform tunable multicasting NRZ-to-RZ format conversion simply by employing multiple cw control waves. Second, it is worth noting that the NRZ differential phase-shift keying (DPSK) signal can also be converted into PRZ signal using the FDI,[15] which provides the possibility of performing NRZ-DPSK-to-RZ-DPSK format conversion. These PPLN-based all-optical format conversions are attractive for all-optical signal processing and may find wide applications for future all-optical networks.

In conclusion, a scheme of all-optical format conversion from NRZ to RZ at 10 and 20 Gbit/s is proposed and demonstrated by using a PPLN waveguide and a RSOA. An FDI is introduced to perform NRZ-to-PRZ format conversion for the purpose of enhancing the clock components. The RSOA-based AMLFRL is utilized to generate the pulsed pump optical clock. The PPLN waveguide is used to complete the NRZ-to-RZ format conversion based on the cSFG/DFG nonlinear interactions. The results imply that tunable operation can be realized simply by changing the cw control wavelength.

This work was supported by the National Natural Science Foundation of China under Grant No. 60577006, and by the program for New Century Excellent Talents in University (NCET-04-0694). The authors would like to thank Y. Yu and J. Xu for their helpful discussions.

[1]C. Langrock, S. Kumar, J. E. McGeehan, A. E. Willner, and M. M. Fejer, J. Lightwave Technol. **24**, 2597 (2006).
[2]C. Q. Xu, H. Okayama, and M. Kawahara, Appl. Phys. Lett. **63**, 3559 (1993).
[3]K. Gallo, G. Assanto, and G. I. Stegeman, Appl. Phys. Lett. **71**, 1020 (1997).
[4]G. P. Banfi, P. K. Datta, V. Degiorgio, and D. Fortusini, Appl. Phys. Lett. **73**, 136 (1998).
[5]I. Cristiani, G. P. Banfi, V. Degiorgio, and L. Tartara, Appl. Phys. Lett. **75**, 1198 (1999).
[6]J. Wang, J. Q. Sun, J. R. Kurz, and M. M. Fejer, IEEE Photonics Technol. Lett. **18**, 2093 (2006).
[7]J. Wang, J. Q. Sun, C. H. Luo, and Q. Z. Sun, Appl. Phys. B: Lasers Opt. **83**, 543 (2006).
[8]S. Ashihara, T. Shimura, K. Kuroda, N. E. Yu, S. Kurimura, K. Kitamura, M. Cha, and T. Taira, Appl. Phys. Lett. **84**, 1055 (2004).
[9]J. Wang, J. Sun, and Q. Sun, Opt. Lett. **31**, 1711 (2006).
[10]J. Wang, J. Q. Sun, and Q. Z. Sun, Opt. Express **15**, 1690 (2007).
[11]J. Wang, J. Q. Sun, and Q. Z. Sun, IEEE Photonics Technol. Lett. **19**, 541 (2007).
[12]J. Q. Sun and J. Wang, Opt. Commun. **267**, 187 (2006).
[13]J. Wang, J. Q. Sun, Q. Z. Sun, D. L. Wang, and D. X. Huang, Opt. Express **15**, 583 (2007).
[14]J. Wang, J. Q. Sun, and Q. Z. Sun, Opt. Lett. **32**, 1477 (2007).
[15]Y. Yu, X. L. Zhang, and D. X. Huang, IEEE Photonics Technol. Lett. **18**, 2356 (2006).